International Journal of Engineering Inventions
e-ISSN: 2278-7461, p-ISSN: 2319-6491
Volume 13, Issue 11 [November. 2024] PP: 106-110

Numerical Simulation For Lithium-Ion Battery Pack Cooled By Serpentine Flow Channel

Nguyen Thanh Cong[1], Tran Duc Hoang[2]
[1,2]*Faculty of Vehicle and Energy Engineering, Thai Nguyen University of Technology,Thai Nguyen, Vietnam*

ABSTRACT: *Due to the advantages of high energy density, no memory effect, and long cycle life, Li-ion batteries are being widely studied and proverbially used as power sources for electric vehicles. Further, along with a few other parameters, the operating temperature of the battery of an electric vehicle plays a vital role in its performance. The operating temperature range of an electric vehicle lithium-ion battery ranges from 15ºC to 35ºC and this is being achieved by a battery thermal management system (BTMS). In the present study, computational analysis for Lithium-ion (LiFePO4 18650) pack to evaluate the maximum temperature. Furthermore, a BTMS is designed for the same using a serpentine flow channel which is indirect contact with the cell surfaces. Water is used as coolant and analysis is carried out for 0.05 m/s velocity rate. The maximum temperatures attained by the cells with and without BTMS are found to be is 304.23 K, 302.68 K, 301.37 K and 316.84 K, 311.11 K, 302.68 K at discharge rates of 1.5 C, 1.0 C and 0.5C, respectively. Therefore, with BTMS the maximum cell temperature attained is 27%, 23% and 3% less compared to the bare cell, which indicates that the BTMS adopted in the present work is significantly effective in controlling rise in cell temperature*

KEYWORDS*: Li-on battery, thermal model, temperature distribution, ECM, ANSYS Fluent*

Date of Submission: 25-10-2024 Date of acceptance: 06-11-2024

I. INTRODUCTION

By virtue of high volumetric and gravimetric energy densities along with no memory effect and long cycle life, Li-ion batteries are being intensively studied and extensively used as power sources for electric vehicle (EV) applications [1]. However, the Li-ion battery performance is highly sensitive to the operational temperature [1], [2]. For example, Li-ion batteries often suffer severe power loss under temperatures below zero degrees Celsius, and face the increased risk of thermal runaway at extremely high temperatures [3]-[5]. Thus, a thermal management system is necessarily required to control the system temperature within a permitted range, and maintain the temperature uniformity throughout the overall system.

Currently, commonly used BTMS are mainly based on air-cooled, liquid-cooled, and phase-change materials. Liquid-cooled BTMS has a higher heat transfer coefficient, and its cooling efficiency is higher. However, liquid-cooled systems are also usually more complex and can have leakage problems. In addition, liquid-cooled systems also tend to be accompanied by higher power consumption. The PCM based approach is a new type of battery thermal management solution. It can effectively control the battery pack temperature in the optimal operating temperature range and ensure excellent temperature uniformity. However, it also has the problems of poor structural strength, leakage of melting material, and low thermal conductivity [6]. The liquid cooling method is the most widely used BTMS method nowadays. Depending on whether the battery pack is in direct contact with the coolant or not, the liquid cooling systems can be divided into two modes: direct contact and indirect contact. Compared with indirect contact BTMS, the cooling performance of direct contact BTMS is slightly better, but indirect contact BTMS is more suitable for practical applications [7]. The cold plate is the most common form of indirect liquid cooling, and the structure and arrangement of the liquid cooling plate are important factors affecting the performance of indirect liquid cooling BTMS [8]. Many related studies have been conducted to improve the cooling performance of the whole system by optimizing the flow channel and structural design of the liquid-cooled plate [9]. Qian et al. [10] proposed an indirect liquid cooling method based on minichannel liquid cooling plate for a prismatic lithium-ion battery pack and explored the effects of the number of channels, inlet mass flow rate, flow direction, and channel width on the thermal performance of this

lithium-ion battery pack using numerical simulation method. Their results showed that the minichannel cold plate thermal management system could control the temperature of the battery pack well under 5C discharge conditions. Zhao et al. [11] simulated and investigated the thermal behavior of a battery module consisting of 71 18650 lithium-ion battery cells under indirect liquid cooling based on channels.

II. MODELING METHOD

2.1 Geometry models of the battery pack

The lithium battery studied in this paper is a cylindrical LiFePO4 battery, the battery model is 18650 which the diameter and height of a single battery are 18 mm and 65 mm, respectively. The rated voltage of each single battery is 4.2 V and the capacity is 1.35Ah. The material of the cooling plate is aluminum. Table 1 shows the thermal physical parameters of the materials of the cooling and heat dissipation system of the lithium battery pack. In Table 1, ρ denotes density, C is heat capacity, k means thermal conductivity, μ represents dynamic viscosity.

Table 1 : Thermal physical parameters of materials for cooling and heat dissipation system

Material	ρ(Kg/m3)	C(J/KgK)	k(W/(mK))	μ(Kg/(ms))
Water	998.2	4128	0.6	1.003 × 10−3
Aluminum	2719	891	202.4	-
Battery	2018	1282	2.7	-

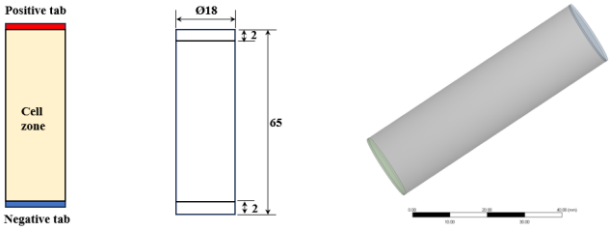

a) b) c)

Fig.1. Lithium-ion cell details a) Cell components b) Cell dimesions c) Single cell model

For formulation, the cell is divided into three main components i.e., anode as negative tab, cathode as positive tab and the middle component as cell zone, the detailed structure is illustrated in Fig.1. In order to simplify the calculation, this paper selects 48 lithium batteries for this design. This kind of cooling and heat dissipation is a serpentine cooling channel which is shown in Fig.2a) and Fig.2 b) shows the 3D models of the lithium battery pack . Coolant (water) flows in from its inlet, passes through the lithium battery pack and then flows out from the outlet to achieve the purpose of cooling and heat dissipation. In the serpentine cooling channel, the thickness of the cooling plate is 3.0 mm and the thickness of the cooling wall is 0.5 mm.

a) 3D model of lithium battery pack b) Serpentine cooling chanel

Fig.2. The structure of the serpentine cooling channel and heat dissipation system

2.2 Numerical Model.

The Reynolds number (Re) of the coolant in the micro channels needs to be determined to determine the flow pattern of the fluid. It is calculated as follows:

$$\mathrm{Re} = \frac{\rho_w u_w d_H}{\mu_w} \tag{1}$$

where ρ_w indicates the density of water, kg/m^3 ;u_w indicates the velocity of water, m/s; d_H indicates the equivalent diameter of the channel, m; μ_w indicates the dynamic viscosity of water, kg/(m·s).

After calculation, it is found that the Reynolds number in the channel is less than 2300, which is a laminar flow. In the simulation, water is assumed to be an incompressible fluid. Its continuity equation is expressed as:

$$\frac{\partial v_x}{\partial x}+\frac{\partial v_y}{\partial y}+\frac{\partial v_z}{\partial z}=0 \tag{2}$$

Its momentum equation is shown as: [12]

$$\frac{\partial}{\partial t}(\rho_w \vec{v}_w)+\nabla.(\rho_w \vec{v}_w \vec{v}_w)=-\nabla p+\mu_w \nabla^2 \vec{v}_w \tag{3}$$

where v_w denotes the velocity vector of the water; where p denotes the static pressure of water,Pa

Its energy equation is shown in equation (5) [13]:

$$\frac{\partial}{\partial t}(\rho_w C_{p,w} T_w)+\nabla.(\rho_w C_{p,w} T_w \vec{v}_w)=\nabla.(k_w \nabla T_w) \tag{4}$$

where $C_{p,w}$ is the specific heat capacity of water under constant pressure, J/(kg·K); k_w is the effective thermal conductivity, W/(m·K).

For the cold plate and the contact thermal resistance layer, the heat transfer process is controlled by the heat transfer differential equation:

$$\rho C_p \frac{\partial T}{\partial t}=\nabla.(k\nabla T) \tag{5}$$

where ρ, C_p, and k denote the density of the corresponding material, kg/m^3 , the constant pressure specific heat capacity, J/(kg·K), and the thermal conductivity, W/(m·K), respectively.

For the cell domain, the heat transfer process is controlled by [14]

$$\rho_b C_{p,b}\frac{\partial T}{\partial t}=\frac{\partial}{\partial x}\left(\lambda_x \frac{\partial T}{\partial x}\right)+\frac{\partial}{\partial y}\left(\lambda_y \frac{\partial T}{\partial y}\right)+\frac{\partial}{\partial z}\left(\lambda_z \frac{\partial T}{\partial z}\right)+Q \tag{6}$$

where ρ_b denotes the density of the cell domain, kg/m^3; $C_{p,b}$denotes the constant pressure specific heat capacity of the cell, J/(kg·K); λ_x, λ_y, and λ_z denote the thermal conductivity of the cell domain in the x, y, and z directions, respectively, W/(m·K); Q denotes the heat generated by the cell during discharge[14] W/m^3.

All inlet boundary conditions in the research are velocity inlet, with constant inlet velocity and inlet temperature of 298K. All outlet boundary conditions are pressure-outlet, with atmospheric pressure at outlet. The fluid walls, as shown in Fig 2, are set as a no-slip wall boundary. All of the outer walls of the model are set as an insulation boundary. The simulations are performed on the ANSYS FLUENT platform. The spatial discretization methods of pressure, momentum, energy, and potential are second order, second order upwind, second order upwind, and first order upwind, respectively. In the simulation, the convergence criteria of velocity, energy, and potential are 10^{-6}.

III. RESULTS AND DISCUSSION

3.1 The influence of discharging rate on the performance of a single battery.

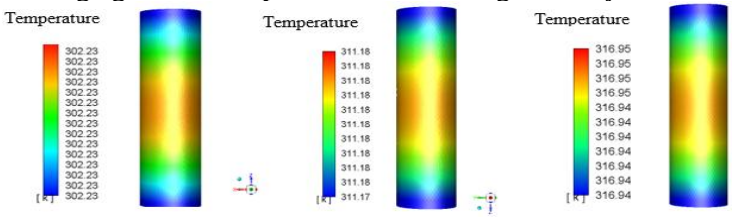

a) 0.5C b) 1.0C c) 1.5C

Fig.3. Temperature contour of the cell at different discharge rates.

The cell behaviour when being discharged at different rates is computed by equation and ECM model. Fig 3 shows the temperature contour of single cell for three different discharge rates 0.5 C, 1.0 C and 1.5 C. The figure demonstrates a symmetric pattern in temperature in the whole cell; however, the discrepancy between temperatures in positive and negative tabs is small.

The maximum temperature for discharge rates 0.5 C, 1.0 C and 1.5 C are 302.23 K, 311.18 K and 316.95 K respectively. The temperature tends to increase over time is represented in Fig 4. The maximum temperature attained by the cell is found to be highest for 1.5 C discharge rate. A comparison of voltage drop at three different discharge modules is shown in Fig 5. It is clear from the graph that as discharge rate increases, temperature as well as voltage drop increase. It is observed that 316.95 K is the maximum temperature attained by the cell at 1.5 C discharge rate due to high internal resistance and the charge is completely drained within 2500 seconds at same discharge rate. At a discharge rate of 1.5 C the cell attains maximum temperature of 316.95 K which exceeds the optimum temperature. Hence, it is important to reduce this temperature by adopting BTMS.

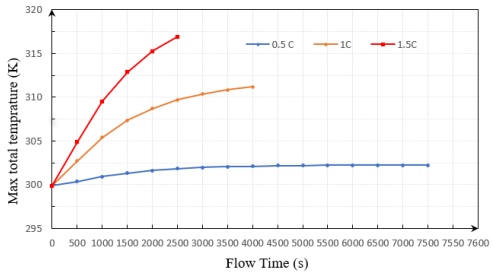

Fig.4. Temperature variation at different discharge rates

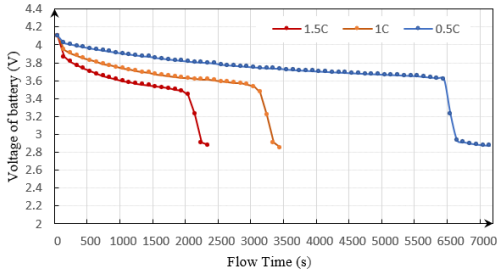

Fig.5. Battery cell voltage variation at different discharge rates

3.2. Battery pack with BTMS.

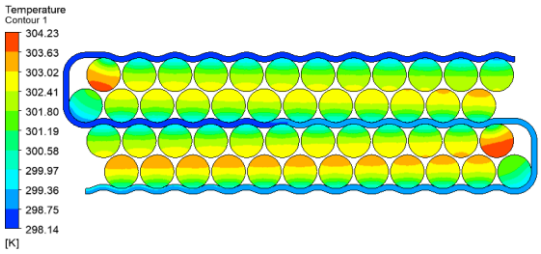

Fig.6. Internal temperature of battery pack at the end of 1.5C

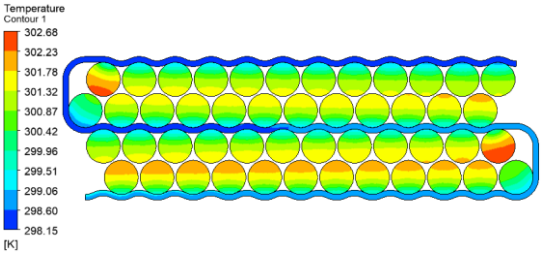

Fig.7. Internal temperature of battery pack at the end of 1.0C

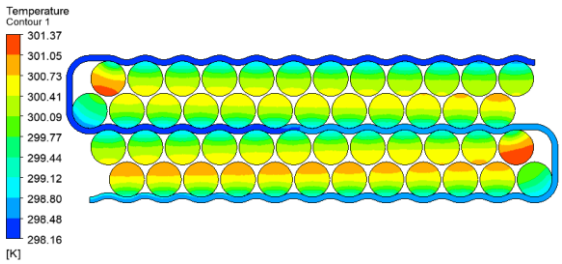

Fig.8. Internal temperature of battery pack at the end of 0.5C

Fig.6-8 show the temperature contour of battery pack with cooled by serpentine flow channel for three different discharge rates 1.5 C, 1.0 C and 0.5 C, the maximum temperature of battery pack with cooling plate for discharge rates 1.5 C, 1.0 C and 0.5 C are 304.23 K, 302.68 K, 301.37K respectively. It can be observed that contact part of the cells with cooling plate is cooler compared to the non-contact part and the temperature difference between these parts is considerably less.

IV. CONCLUSIONS

In the present work CFD analysis has been carried out on battery pack 18650 LiFePO4 for electric vehicle application. The variation of cell temperature with time without cooling has been evaluated at different discharge rates of 0.5 C, 1.0 C and 1.5 C. Furthermore, a BTMS by serpentine flow channel with water as coolant has been used to regulate the maximum temperature attained by the cell. Maximum temperature attained by the cell with and without cooling has been simulated at various constant current discharge rates. The outcome of the simulation study is summarized below:

- Battery pack without cooling attains maximum temperature of 316.95 K, 311.18 K, 302.23 K at discharge rates of 1.5 C, 1.0 C and 0.5 C respectively.

- Battery pack with BTMS it is observed that the maximum temperature attained by the cell is 304.23 K, 302.68 K, 301.37 K at discharge rate of 1.5 C, 1.0 C and 0.5 C respectively.

- Compared to bare cell, the cell with BTMS reduces temperature reached by 27%, 23% and 3% at discharge rates of 1.5 C, 1.0 C and 0.5 C respectively thus implying that the BTMS adopted in the present study is effective.

Acknowledgment

The authors wish to thank the Thai Nguyen University of Technology for supporting this work.

REFERENCES

[1]. X. Hu, J. Jiang, D. Cao, and B. Egardt, ‘‘Battery health prognosis for electric vehicles using sample entropy and sparse Bayesian predictive modeling,’’ IEEE Trans. Ind. Electron., vol. 63, no. 4, pp. 2645–2656, Apr. 2016.
[2]. C.-Y. Wang et al., ‘‘Lithium-ion battery structure that self-heats at low temperatures,’’ Nature, vol. 529, pp. 515–518, Jan. 2016.
[3]. M. Armand and J.-M. Tarascon, ‘‘Building better batteries,’’ Nature, vol. 451, no. 7179, pp. 652–657, 2008.
[4]. X. Feng et al., ‘‘Characterization of penetration induced thermal runaway propagation process within a large format lithium ion battery module,’’ J. Power Sources, vol. 275, pp. 261–273, Feb. 2015.
[5]. X. Feng et al., ‘‘Thermal runaway propagation model for designing a safer battery pack with 25 Ah LiNixCoyMnzO2 large format lithium ion battery,’’ Appl. Energy, vol. 154, pp. 74–91, Sep. 2015.
[6]. W. Wu, S. Wang, W. Wu, K. Chen, S. Hong, and Y. Lai, “A critical review of battery thermal performance and liquid based battery thermal management,” Energy Conversion and Management, vol. 182, pp. 262–281, 2019.
[7]. D. Chen, J. Jiang, G.-H. Kim, C. Yang, and A. Pesaran, “Comparison of different cooling methods for lithium ion battery cells,” Applied Thermal Engineering, vol. 94, pp. 846–854, 2016.
[8]. J. Wang, S. Lu, Y. Wang, C. Li, and K. Wang, “Effect analysis on thermal behavior enhancement of lithium-ion battery pack with different cooling structures,” Journal of Energy Storage, vol. 32, article 101800, 2020.
[9]. W. Zichen and D. Changqing, “A comprehensive review on thermal management systems for power lithium-ion batteries,” Renewable and Sustainable Energy Reviews, vol. 139, article 110685, 2021
[10]. Z. Qian, Y. Li, and Z. Rao, “Thermal performance of lithium-ion battery thermal management system by using mini-channel cooling,” Energy Conversion and Management, vol. 126, pp. 622–631, 2016.
[11]. C. Zhao, W. Cao, T. Dong, and F. Jiang, “Thermal behavior study of discharging/charging cylindrical lithium-ion battery module cooled by channeled liquid flow,” International Journal of Heat and Mass Transfer, vol. 120, pp. 751–762.
[12]. G. K. Batchelor, An introduction to fluid dynamics, Cambridge University Press, 2000.
[13]. A. Bejan, Convection heat transfer, John Wiley & Sons, 2013.
[14]. S. C. Chen, C. C. Wan, and Y. Y. Wang, “Thermal analysis of lithium-ion batteries,” Journal of Power Sources, vol. 140, no. 1, pp. 111–124, 2005.